Leaky atomic traps: Upward diffusion of Au from nanoscale pits on ionic-crystal surfaces

M. Goryl,[1] F. Buatier de Mongeot,[2] F. Krok,[1] A. Vevecka-Priftaj,[3] and M. Szymonski[1,*]

[1]*Center for Nanometer-Scale Science and Advanced Materials (NANOSAM), Faculty of Physics, Astronomy, and Applied Computer Science, Jagiellonian University, ulica Reymonta 4, 30-059 Krakow, Poland*

[2]*Dipartimento di Fisica, Università di Genova, Via Dodecaneso 33, 16146 Genova, Italy*

[3]*Department of Physics, Polytechnic University of Tirana, Sheshi "Nene Tereza," No. 4, Tirana, Albania*

(Received 8 March 2007; revised manuscript received 21 May 2007; published 17 August 2007)

We have investigated the formation of gold nanoclusters during submonolayer deposition on atomically flat KBr and RbI (001) ionic-crystal substrates, as well as on substrates patterned with two-dimensional (2D) nanoscale pits produced by electron stimulated desorption. In this way, it is possible to produce atomic steps free from stress and local charging, which are normally considered the reason for enhanced cluster nucleation. Easy nucleation of the Au clusters inside the pits at the lower side of the atomic step edge is not observed, while nucleation of the Au nanoclusters is found to occur preferentially at the upper step edges. Moreover, we observe that gold atoms landing inside the bottom of the pits are able to escape from them by means of thermally activated upward diffusion at the step edges. We propose that the preferential Au nucleation sites at the edges of 2D pits are activated by F centers produced in electronic processes used for nanopatterning of the ionic crystals.

DOI: 10.1103/PhysRevB.76.075423 PACS number(s): 68.55.Ac, 81.16.Rf, 68.37.Ps

I. INTRODUCTION

The possibility to finely tune the morphology of an epitaxial thin film by controlled kinetic manipulation during self-assembly and physical vapour deposition (PVD) deposition is of great potential interest in many technological prospects, among which we can mention quantum dots and semiconductor heterostructures, metal films, wires, and dots for applications in electronic, magnetic, and optoelectronic devices.[1,2] In this context, application of electronic excitations for nanofabrication of two-dimensional (2D) pits on surfaces of ionic insulators[3–5] has recently attracted increasing attention, despite the fact that fundamentals of desorption induced by electronic transitions were studied already for several decades.[6–8] One of the main atomistic processes, which has to be controlled for achieving either the growth of flat films or the formation of self-organized nanostructures, is the traversal of atomic step edges via activated diffusion. In the conventional picture which has been developed for metal-metal epitaxy, an atom approaching an atomic step from the upper side feels an extra barrier [Ehrlich-Schwoebel barrier (ES)][9,10] when attempting to cross a step edge, so that at sufficiently low temperatures, preferential attachment occurs at the ascending step edges, where atom coordination is increased. A particularly interesting class of systems is that of metal clusters supported on insulating or ionic nanostructured substrates, e.g., for their optical, magnetic, and catalytic applications.[11,12] For example, gold nanoclusters of sizes around 2–3 nm were demonstrated to be remarkably active in low temperature oxidation reactions, though in bulk form, gold is the least reactive among the noble metals.[13]

The role of heterogeneous nucleation of metal islands and clusters at defects on terraces[14] and particularly at step edges of cleaved surfaces[11,12,15] has been evidenced in several instances. Cleavage is the standard way of preparing atomically well defined ionic-crystal substrates; however, it introduces highly localized stress fields and residual charging localized at step edges,[11] which is suspected to be one of the reasons for the preferential nucleation at step edges on these substrates. In order to evidence the role of edge defects, stress fields, and charging in cluster nucleation at step edges, we developed a procedure based on electron irradiation which allows us to pattern *in situ* the substrate with nanoscale pits bound by monatomic steps free from stress and charging and with a well defined low density of kink and corner sites.[16,17] These substrates have then been used as templates for the subsequent deposition of metal clusters under well defined conditions. One of the ideas driving this experiment was the possibility of obtaining the selective nucleation of gold *into* the nanopits with the aim of forming laterally confined nanoscale metal electrodes for perspective applications in molecular electronics. Such possibility has been proposed in a recent letter by Mativetsky *et al.*[5] in which Ta atoms were codeposited from an electron beam evaporator on patterned KBr surfaces.

In this paper, we report on observations made after Au deposition on flat KBr(001) and RbI(001) terraces and on 2D nanoscale pits obtained by electron (or UV in RbI case) irradiation of the atomically flat substrates, which provide evidence contrary to the prevailing expectations. In particular, we have observed not only that cluster nucleation preferentially took place at the upper edge of a pit step, an observation which is not uncommon in other metal–ionic-crystal systems, but also that Au atoms trapped inside the 2D nanoscale pits were able to escape from them at room temperature via true-upward diffusion events taking place at the monoatomic high ⟨001⟩ steps of KBr.

II. EXPERIMENT

The experiment has been performed in an ultrahigh vacuum (UHV) system consisting of three chambers (sample preparation, surface analysis, and scanning probe microscope). The chambers are interconnected, and samples can be

prepared and transferred by magnetically coupled linear transfers in UHV. The base pressure in the system is below 5×10^{-11} Torr. KBr crystals, purchased from Kelpin Crystals (Neuhausen, Germany), are cleaved in air parallel to the (001) cleavage plane of KBr and immediately transferred into the vacuum system for annealing. The crystal kept at temperature of 400 K is irradiated with a 1 keV electron beam scanned over an area of ~1 cm^2, with average current of 1 μA and a spot size of ~0.5 mm. The gold evaporation is carried out with rate of 0.1 ML/min (where ML stands for a monolayer of gold) at a sample temperature of $T=295$ K using a resistive heating evaporator with a quartz-crystal microbalance as flux monitor. Imaging is performed with modified VP2 AFM/STM Park Scientific Instruments microscope operating at room temperature. All images are obtained in a noncontact atomic force microscopy (NC-AFM) frequency modulation mode with the use of Nanosourf "easyPLL" demodulator. Commercially available silicon (boron-doped) piezoresistive cantilevers are used as probes. The resonant frequencies of the cantilevers are typically about 250 kHz and the spring constant is 20 N/m. Detunings, i.e., frequency shifts of the interacting cantilever with respect to its resonant frequency, are set in the range of 10–50 Hz at constant oscillation amplitudes of 60–100 nm. The scanning rates are 0.4–1 scan line/s.

III. RESULTS AND DISCUSSION

In Fig. 1(a), a typical KBr(001) substrate after cleavage in air followed by annealing in UHV at 550 K for several hours is shown. The annealing procedure is necessary in order to remove the adsorbed impurities and to reduce the stress and charging accumulated during the cleavage process, as was pointed out previously (see, e.g., Refs. 18 and 19). The images show that extended atomic terraces with typical sizes exceeding 300 nm separated by monatomic steps are formed. The step contour is wavy, indicating that a non-negligible amount of kinks is present; moreover, in the AFM images, the local contrast over the step edges is stronger. Barth and Henry suggested that defects, or residual local charging, could be present at step edges even after annealing.[11,19] Moreover, it is very often in noncontact AFM that ions at edges are imaged as much brighter than the ions on flat terraces due to surface atom relaxation[20,21] under the tip approach. Since the edge atoms have a lower coordination number and thus are more weakly bound to the surface, their relaxation is much stronger than the relaxation of atoms in a flat terrace.

Deposition of submonolayer amounts of Au on such terraces has then been performed at a constant flux of 0.3 ML/min (1 ML equivalent to 1.38×10^{15} atoms/cm^2) at a substrate temperature $T=300$ K. In Fig. 1(b), a NC-AFM topography shows that after deposition of 0.1 ML Au, the surface appears decorated by one-dimensional chains of clusters, which nucleate along the step contours. Under these deposition conditions, terrace nucleation becomes competitive with step nucleation when the terrace width exceeds approximately 60 nm. We stress that direct imaging of individual metal clusters supported on ionic-crystal substrates by means of NC-AFM is a delicate, nontrivial experimental task, since local electrostatic interactions probably due to charging of the metal cluster[11,12,19] result in broadening of the topographic features. Also, tip convolution effects have to be taken into account, especially when imaging steep clusters. However, cluster density and their lateral positions can be reliably extracted from the AFM topographies. An estimate of the Au cluster diameter can be made by taking into account the cluster density and the amount of Au deposited, which yields a value peaked around 2 nm. Such a cluster size is in an interesting range, as demonstrated by experiments on supported Au clusters, which show unexpectedly high reactivity with respect to low temperature CO oxidation.[13]

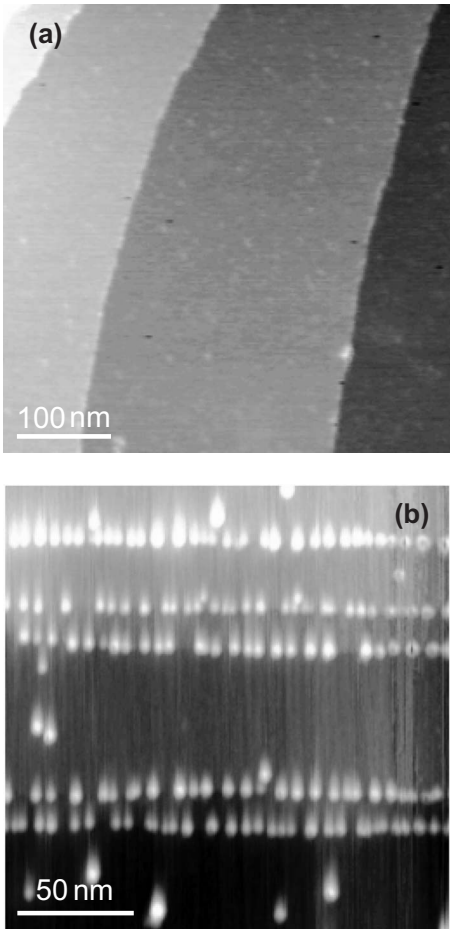

FIG. 1. (a) NC-AFM topography of a KBr(001) cleaved substrate after vacuum annealing. The image exhibits monoatomic high steps separating atomically flat terraces (vertical range, 1 nm; image size, 500×500 nm^2). (b) NC-AFM topography of a KBr(001) cleaved substrate after deposition of 0.1 ML of Au (flux of 0.3 ML/min) at a substrate temperature $T=300$ K (vertical range, 2 nm; image size, 200×200 nm^2).

An estimate of the linear density of the clusters nucleated at steps after deposition of Au at 300 K turns out to be 0.14 nm^{-1}, corresponding to an average cluster separation of about 7 nm. The observation of such densely packed linear arrays of metal clusters is rather the rule than the exception, as it was also reported for closely related systems Fe/NaCl,[22] Pd/MgO(001),[14] Au/MgO(001).[23] The common rationale for these observations, all made on cleaved substrates, could

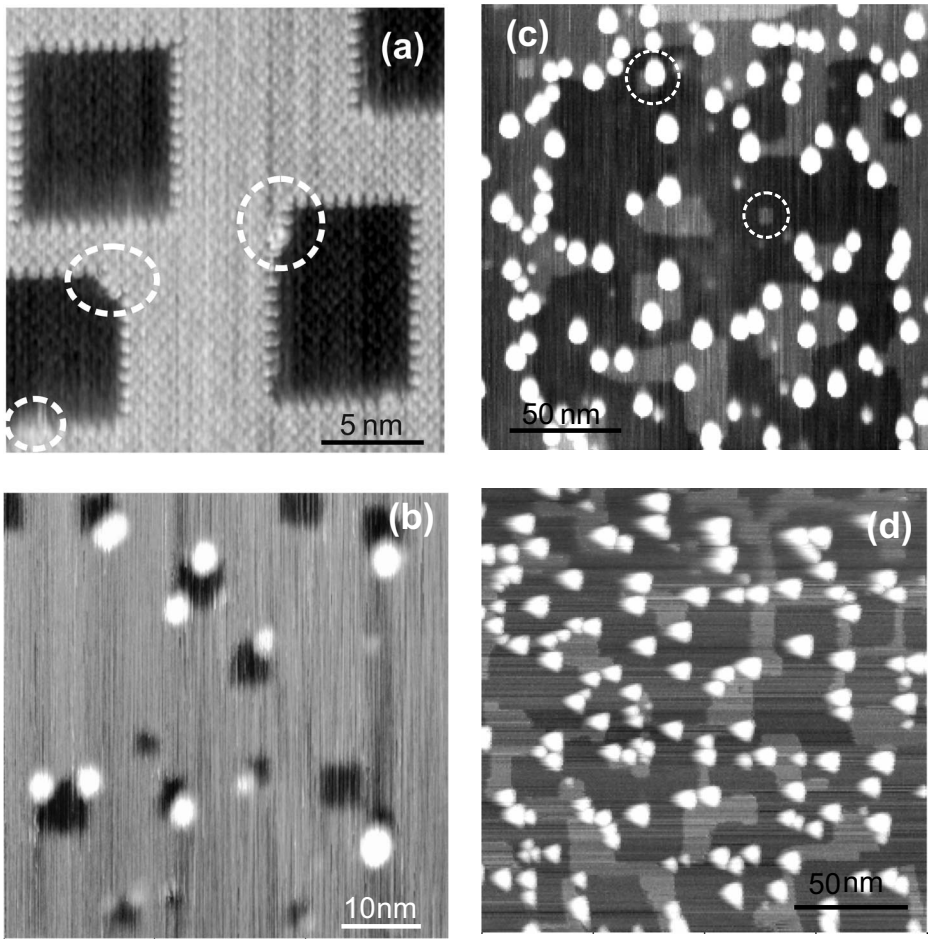

FIG. 2. (a) NC-AFM topography of an atomically resolved KBr(001) terrace after exposure to 1 keV electrons. Nanoscale pits bound by [001] steps are formed (vertical range, 0.35 nm; image size, 22×22 nm^2). (b) NC-AFM topography of a KBr(001) substrate patterned with nanoscale pits after deposition of 0.1 ML of Au at room temperature (saturated vertical range, 0.5 nm; image size, 60×60 nm^2). (c) NC-AFM topography of a KBr(001) substrate patterned with nanoscale pits after deposition of 0.1 ML of Au at room temperature (saturated vertical range, 0.9 nm; image size, 200×200 nm^2). (d) NC-AFM image of RbI (001) surface irradiated with UV light ($\lambda\geqslant200$ nm) at sample temperature of 380 K after deposition of 0.1 ML of Au at room temperature (saturated vertical range, 1.6 nm; image size, 200×200 nm^2).

be connected to the possibility that following cleavage, atomic steps are affected by a high density of uncontrolled defects and by local charging, as has been recently proposed in Ref. 19. The defects could, in turn, act as preferential heterogeneous nucleation sites,[14] and this could be the case also in the present experiment, since the linear cluster density along cleavage steps does not change significantly when Au deposition is performed at 400 K.

With the aim of understanding cluster nucleation at atomic step edges under controlled conditions, we performed Au deposition experiments on KBr substrates prepatterned *in situ* by electron irradiation. In Fig. 2(a), we present an atomically resolved KBr(001) terrace after exposure to 1 keV electrons. The latter process results in the formation of monolayer-deep square nanoscale pits with atomically well defined step edges running along the nonpolar [110] and [1 −10] directions. Most importantly for the present context, the steps bounding the artificial pits are not affected by the local stress, charging, and contamination which are invariably present after mechanical cleavage,[21] since in the present case, the generation of new atomic steps proceeds by surface segregation of activated defects (F centers) produced in the near-surface layers by the energetic electrons.[16,18]

When an electron with energy higher than the band gap energy (in the order of 10 eV for halides) reaches the alkali halide crystal, it causes creation of hot-electron–hole pairs by inelastic interactions with the crystal lattice.[6–8] The electrons and holes could efficiently migrate to the surface via uncorrelated diffusion of the conduction band electron and the hole having an excess of kinetic energy. The surface recombination of the pair occurs with prompt emission of nonthermal halogen and creation of the surface F center.[6] Alternatively, the electron-hole pair could self-trap leading to the production of the Frenkel pairs (so called F-center and H-center pair of defects).[7,8] Diffusion of these defects in the vicinity of the surface can lead to thermal desorption of crystal constituents. H center migrating to the surface produces a halogen adatom.[6] Since the binding energy of such an atom is relatively low (0.14 eV), it leaves the surface easily even at room temperature. The behavior of a F center depends on its electronic state. F centers in the ground state are rather immobile at room temperature and can be accumulated in the vicinity of the crystal surface. However, those excited by light or by irradiating electron beam become highly mobile[24,25] and could have sufficient energy to neutralize and desorb an alkali atom from low-coordinated surface lattice sites such as steps and kinks. The accumulation of ground-state F centers, together with the preferential desorption from low-coordinated sites on the surface, plays an essential role in explaning of the 2D pit formation on irradiated surfaces of alkali halides.[25]

A statistical analysis on a large number of images shows that the atomic steps so produced are invariably aligned along the high symmetry directions and present a very low density of kinks, which are clearly imaged in the atomically resolved topographies [Fig. 2(a)]. The kinks appear to be the

only kind of low coordination defects which can be imaged on the steps produced by electron irradiation. An estimate of the linear kink density in steps produced by electron irradiation turns out to be 3×10^{-2} nm^{-1}, i.e., almost an order of magnitude less than the linear cluster density observed at cleaved steps [Fig. 1(b)]. We underline that the two-dimensional pits provide a "relative" local topographic minimum which is ideally suited for studying Au nucleation in a confined geometry bound by a connected contour of ascending steps. Figure 2(b) shows the outcome of a submonolayer Au deposition experiment on a substrate prepatterned under conditions equivalent to those of Fig. 2(a). To our surprise, the outcome of the growth experiment does not provide any clear evidence for gold confinement *inside* the pits. One obvious observation could be that no Au nucleation takes place into the pits because the amount of material deposited into them is insufficient [under the deposition conditions of Fig. 2(b), about 35 Au atoms are deposited on average within each pit of average size of 5×5 nm^2]. Thus, instead of increasing the Au coverage, in order to avoid degradation of the imaging resolution in the presence of high density of clusters, we decided to prepattern the KBr substrate with pits with a larger size of the bottom terrace by increasing the electron irradiation dose to 10 μC/cm^2. In this way, pit sizes of about 50×50 nm^2 are formed, which compares well to the extension of the denuded zone observed after gold deposition on a flat cleaved substrate [Fig. 1(b)]. Thanks to the increased capture area, now the square pits receive about 3500 atoms after a 0.1 ML Au deposition dose, i.e., an amount sufficient to form about ten clusters of nominal average size on an area of approximately 50×50 nm^2. Instead, after deposition of 0.1 ML Au [Figure 2(c)], we again find that nucleation takes place almost exclusively at the upper terraces. The cluster density within the bottom of the extended pits is now about 2.1×10^{10} cm^{-2}, i.e., about 1 order of magnitude lower than the nucleation density on the extended terraces produced after cleavage under conditions equivalent to Fig. 1(b) (1.7×10^{11} cm^{-2}). We stress that the above given cluster densities inside the pits are to be considered as *upper bounds*, since small supporting KBr islands [see circles in Fig. 2(c)] are left behind after electron irradiation and are not visible in the dynamic force microscopy images when a gold cluster resides over them. A statistical analysis of the images shows that only about 17% of the clusters are nucleated at the bottom of the pits, while the remaining 73% are supported at the upper step side with an undetermined 10% fraction. The statistical uncertainty of this analysis is estimated as equal to ±5%. Taking into account that as much as 57% of the surface area shown in Fig. 2(c) is covered by the pits, we have to conclude that even at room temperature, significant upward mass transport is active from the bottom of the pits to the upper terraces, where nucleation preferentially takes place near the upper step edges which act as efficient trapping sites. We stress here that the availability of an artificial template, the two-dimensional pits acting as local topographic minima which expose a bottom terrace bound by a connected ascending step, proves essential in demonstrating the occurrence of upward diffusion of the Au atoms. The latter effect could not be evidenced in the previously cited examples which showed nucleation at the upper step edge, since in those cases, the substrates presented a random sequence of up-down terraces. This conclusion is further demonstrated if we consider the density of clusters nucleated on the top terrace of a KBr island supported in the middle of a pit in Fig. 2(c). Here, the density of clusters is approximately 1.2×10^{12} cm^{-2}, i.e., a factor of 10 *higher* than the cluster density in the middle of extended terraces [Fig. 1(c)] and a factor of 70 higher than the density of clusters in the bottom of the pits. This second argument further reinforces the conclusion that atoms landing on the underlying pit are able to diffuse toward the edge of the island and, most surprisingly, climb upward where they are trapped in a local minimum near the upper step edge.

The concept of true-upward diffusion during metal on metal epitaxy has already been pointed out clearly in the case of Al/Al(110) deposition.[26] First principles calculations, as well as kinetic Monte Carlo simulations, allowed us to generalize the conclusions to the broader class of fcc (110) substrates[27] and moreover shed light on the key atomistic processes which are responsible for the frequent uphill diffusion events involving an exchange process in which an adatom approaching the step from the lower side is able to get incorporated into the atomic step row displacing an atom upward into the upper terrace. This scenario is, however, at variance with the present context of metal diffusion on an ionic crystal, a prototypical nonmixing epitaxy pair, since we should rule out the occurrence of exchange processes with low activation energy in which a Au adatom gets incorporated into a KBr or RbI step. Rather, the search of low energy pathways for activated diffusion of Au atoms (or even of small clusters) at regular or defective step sites has to proceed with the aid of total energy calculations in order to assess the energetic landscape for adatoms approaching a step edge. Our experimental results provide a clear evidence that the barrier for Au to climb the step edge is small and quite accessible even at room temperature.

Attempts to achieve atomic resolution both on the KBr substrate and on the Au clusters did not prove successful, similar to the previously reported case;[11,19] however, from atomically resolved images resolving the atomic structure of the KBr substrate such as the one shown in Fig. 3, we could unequivocally assess the location of the cluster binding location on the top terraces next to the step sites. Figure 3(b) moreover shows that even on a region where KBr exposes a multilayer high step distribution, Au clusters can be found to be confined on the very top layer, thus suggesting that the majority of atoms which are deposited on lower KBr terraces are able to climb uphill.

If we attempt to reconcile the present observations with the conventional picture derived from metal epitaxy, the energy landscape for an atom diffusing in the neighborhood of a step edge can be sketched recurring to the diagram of Fig. 4(a). The atom approaching the step edge from the upper side, when attempting step traversal, has to overcome an extra energy barrier E_{ES} (Ehrlich-Schwoebel barrier).[9,10] If the atom is able to overcome the step edge, reaching the lower ridge, in general, it experiences an extra binding E_{ls} due to the increased coordination present there. In turn, the residence time of adatoms at the lower step edge is increased and results in a higher nucleation probability at the *lower*

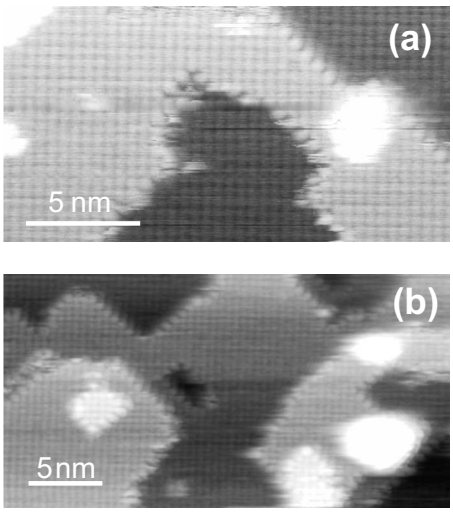

FIG. 3. (a) Atomically resolved NC-AFM image of a KBr(001) substrate patterned by electron irradiation with nanoscale pits after low temperature deposition of 0.1 ML of Au and annealing at room temperature (saturated vertical range, 0.8 nm; image size, 30 $\times 16$ nm^2). (b) Atomically resolved NC-AFM topography of a KBr(001) substrate patterned by electron irradiation with nanoscale pits after low temperature deposition of 0.1 ML of Au and annealing at room temperature (saturated vertical range, 0.8 nm; image size, 20×11 nm^2)

step edge. If we now consider an adatom approaching the step edge from the lower terrace, we will find that, according to the scheme of Fig. 4(a), in order to traverse the step in the upward direction, it will have to overcome an additional activation barrier $E_{ls}+E_{ES}$, which makes the true-upward diffusion event more unfavorable, unless atomic exchange processes at the step edge are active.[26] This last possibility can generally be excluded in the case of metal epitaxy on ionic-crystal substrates. The existence of lower energy pathways for upward diffusion (e.g., localized at kinks which are the only defects evidenced in atomic resolution images) has to be demonstrated by total energy calculations.

The observations of the present experiment, and similar ones for closely related metal-ionic-crystal systems,[28] show

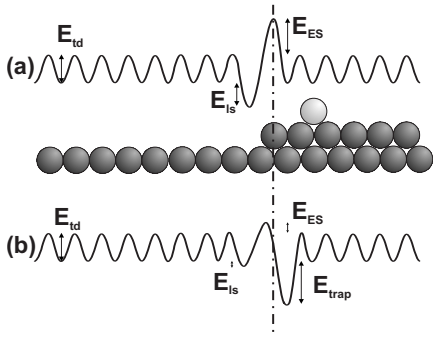

FIG. 4. Schematic potential energy diagram for a Au adatom approaching an atomic step via thermally activated diffusion (E_{td}). In (a), we show a system endowed with a conventional Ehrlich-Schwoebel barrier (E_{ES}) and with trapping at the lower step edge (E_{ls}), and in (b), a system endowed with a reduced ES barrier and strong defect trapping (E_{trap}) near the upper edge of the atomic step.

that a different description should be adopted since a strong tendency for cluster nucleation at the upper side of the step edge is found. From a qualitative viewpoint, the energy diagram should be modified as in Fig. 4(b): The atom approaching the step edge from the upper terrace finds a favorable adsorption site at the upper step edge with an extra binding energy E_{trap}, resulting in increased residence time and nucleation. Such specific attractive sites could be provided by the F centers created in the electron stimulated process of pit creation and localized in the edge vicinity as discussed above. We believe that the accumulated surface F centers could arrange themselves along the step edges of the pits, since the low-coordinated sites are energetically more favorable for them in comparison with the flat surface areas.[12] In fact, recent calculations by Pakarinen *et al.*[12] show that the adhesion energy of an individual Au atom to a step F center filled with another gold atom is as high as 3.7 eV in comparison with only 0.77 eV over the plain surface. For clusters of 25 Au atoms, the adhesion energies are equal to 4.86 eV over the F center, or the F center filled with Au atom, whereas only 3.01 eV above the step edge without the F-center site. Furthermore, we have to stress that individual F centers (i.e. an electron occupying a halogen vacancy site) could not be visualized with dynamic force microscopy on ionic surfaces, since they are essentially not distinguishable from the negative halogen ion network interacting with AFM tip via electrostatic forces.

In order to undertake step traversal in the downward direction, the atom has to overcome an extra energy barrier $E_{ES}+E_{trap}$. On the other hand, since no preferential nucleation is found at the lower edge, we can conclude that the depth of the extra barrier E_{ls} is negligible compared to the thermal energy KT available near room temperature. At the same time, since the data demonstrate that step traversal in the upward direction occurs easily at room temperature, we can conclude that the extra barrier $E_{ls}+E_{ES}$ is small compared to KT.

We should remark that the present picture is not straightforward, since several calculations show that metal nucleation and binding is rather expected to be enhanced at the lower step sites in the case of ideal step terminations.[29] Furthermore, several publications have focused on the importance of terrace defect sites (F centers, or divacancies) for binding on a broader class of systems, e.g., for nucleation of Pd metal clusters on terrace sites in MgO.[30] Defect controlled terrace nucleation was experimentally demonstrated on the same system,[14] as well as for Au on MgO(001).[31]

An issue which should be addressed concerns the generality of the present findings. We have conducted experiments on other metal–ionic-crystal pair choosing, in particular, the growth of Au on RbI(001), since the latter substrate, similarly to KBr, following UV-photon irradiation develops well defined size controlled nanoscale pits. After irradiation of a RbI(001) substrate held at 380 K, the average nanoscale pit extension is peaked around 50–60 nm, with step edges running along nonpolar ⟨100⟩ orientations. Gold deposition (0.1 ML) was then performed on such substrate held at room temperature [Fig. 2(d)]. Nucleation of Au clusters of very regular size appears to proceed preferentially at the upper side of the step edges. A quantitative statistical analysis per-

formed on several patterns allows us to assess that about 59% of the clusters are nucleated at the upper step edge, about 21% inside the nanoscale pits, with a 19% fraction of the clusters having uncertain attribution. The statistical uncertainty of this analysis is estimated as equal to ±5%. Taking into account that as much as 60% of the surface area shown in Fig. 2(d) is covered by the pits, these numbers compare significantly well with those found for Au/KBr, confirming that the conclusions made for the latter system have a general validity for a broader class of systems.

In conclusion, we can summarize our observations as follows: (i) the nucleation of metal clusters preferentially takes place at the upper edge of a (001) step formed either by cleavage of the crystal or electronic excitation of its originally flat surface and (ii) Au atoms trapped inside the 2D nanoscale pits are able to escape from them at room temperature via true-upward diffusion events taking place at the monoatomic high ⟨001⟩ steps of crystal. The present observations, done for the Au-KBr and Au-RbI epitaxy pairs, which could represent a prototypical model system for non-mixing heteroepitaxy, indicate the importance of elementary defects in alkali halides, i.e., F centers which are likely to be preferentially localized at the upper step edges of the crystal and could act as nucleation centers for gold clusters of a well defined size range.

ACKNOWLEDGMENTS

This work was supported by the European Commission within the Integrated Project "Computing Inside Single Molecule Using Atomic Scale Technologies, Pico-Inside," Contract No. 015847, and the Polish Ministry of Science and Higher Education. Four of us (F.B.M. F.K., A.V.-P., and M.S.) wish to acknowledge the support of the EC under Contract No. MTKD-CT-2004-003132, 6th FP-Marie Curie action for Transfer of Knowledge: "Nano-engineering for Expertise and Development-NEED." F.B. acknowledges the financial support of Italian MIUR through FIRB04-RBNE-033KMA projects.

*ufszymon@cyf-kr.edu.pl

[1] *Nanoelectronics and Information Technology*, 2nd ed., edited by Reiner Waser (Wiley, New York, 2005).
[2] *Growth and Properties of Ultrathin Epitaxial Layers*, edited by D. A. King and D. P. Woodruff, The Chemical Physics of Solid Surfaces and Heterogeneous Catalysis Vol. 8 (Elsevier, Amsterdam, 1997).
[3] L. Nony, E. Gnecco, A. Baratoff, A. Alkauskas, R. Bennewitz, O. Pfeiffer, S. Maier, A. Wetzel, E. Meyer, and C. Gerber, Nano Lett. **4**, 2185 (2004).
[4] L. Nony, R. Bennewitz, O. Pfeiffer, E. Gnecco, A. Baratoff, E. Meyer, T. Eguchi, A. Gourdon, and C. Joachim, Nanotechnology **15**, S91 (2004).
[5] J. M. Mativetsky, Y. Miyahara, S. Fostner, S. A. Burke, and P. Grutter, Appl. Phys. Lett. **88**, 233121 (2006).
[6] M. Szymonski, K. Dan. Vidensk. Selsk. Mat. Fys. Medd. **43**, 495 (1993).
[7] K. S. Song and R. T. Williams, *Self-trapped Excitons* (Springer, Berlin, 1993).
[8] N. Itoh and A. M. Stoneham, *Materials Modification by Electronic Excitation* (Cambridge University Press, Cambridge, 2000).
[9] G. Ehrlich and F. G. Hudda, J. Chem. Phys. **44**, 1039 (1966).
[10] R. L. Schwoebel, J. Appl. Phys. **40**, 614 (1969).
[11] C. Barth and C. R. Henry, Nanotechnology **15**, 1264 (2004).
[12] O. H. Pakarinen, C. Barth, A. S. Foster, R. M. Nieminen, and C. R. Henry, Phys. Rev. B **73**, 235428 (2006).
[13] M. Valden, X. Lai, and D. W. Goodman, Science **281**, 1647 (1998).
[14] G. Haas, A. Menck, H. Brune, J. V. Barth, J. A. Venables, and K. Kern, Phys. Rev. B **61**, 11105 (2000).
[15] J. A. Venables and J. H. Harding, J. Cryst. Growth **211**, 27 (2000).
[16] B. Such, J. Kolodziej, P. Czuba, P. Piatkowski, P. Struski, F. Krok, and M. Szymonski, Phys. Rev. Lett. **85**, 2621 (2000).
[17] M. Szymonski, J. J. Kolodziej, B. Such, P. Piatkowski, P. Struski, P. Czuba, and F. Krok, Prog. Surf. Sci. **67**, 123 (2001).
[18] M. Goryl, B. Such, F. Krok, K. Meisel, J. J. Kolodziej, and M. Szymonski, Surf. Sci. **593**, 147 (2005).
[19] C. Barth and C. R. Henry, Nanotechnology **17**, S155 (2006).
[20] R. Bennewitz, A. S. Foster, L. N. Kantorovich, M. Bammerlin, Ch. Loppacher, S. Schar, M. Guggisberg, E. Meyer, and A. L. Shluger, Phys. Rev. B **62**, 2074 (2000).
[21] R. Bennewitz, S. Schaer, V. Barwich, O. Pfeiffer, E. Meyer, F. Krok, B. Such, J. J. Kolodziej, and M. Szymonski, Surf. Sci. Lett. **474**, L197 (2001).
[22] Z. Gai, G. A. Farnan, J. P. Pierce, and J. Shen, Appl. Phys. Lett. **81**, 742 (2002).
[23] R. Bennewitz, J. Phys.: Condens. Matter **18**, R417 (2006).
[24] O. Salminen, P. Riihola, A. Ozols, and T. Viitala, Phys. Rev. B **53**, 6129 (1996).
[25] M. Szymonski, A. Droba, M. Goryl, J. J. Kolodziej, and F. Krok, J. Phys.: Condens. Matter **18**, S1547 (2006).
[26] F. Buatier de Mongeot, W. Zhu, A. Molle, R. Buzio, C. Boragno, U. Valbusa, E. G. Wang, and Z. Zhang, Phys. Rev. Lett. **91**, 016102 (2003).
[27] W. Zhu, F. B. de Mongeot, U. Valbusa, E. G. Wang, and Z. Zhang, Phys. Rev. Lett. **92**, 106102 (2004).
[28] R. Kern and M. Krohn, Phys. Status Solidi A **116**, 23 (1989).
[29] J. Nakamura, T. Kagawa, and T. Osaka, Surf. Sci. **389**, 109 (1997).
[30] L. Giordano, C. Di Valentin, J. Goniakowski, and G. Pacchioni, Phys. Rev. Lett. **92**, 096105 (2004).
[31] K. Hojrup-Hansen, S. Ferrer, and C. R. Henry, Appl. Surf. Sci. **226**, 167 (2004).